Update on the Storage Ring Vacuum System for SPring-8-II

S. Takahashi, M. Oishi, M. Shoji, K. Tamura, Y. Taniuchi, T. Bizen

Overview of SPring-8-II

	SPring-8-II	SPring-8
Beam Energy (GeV)	6	8
Ring Current (mA)	200	100
Unit-cell Structure	5-Bend Achromat	Double-Bend
Length of ID straight (m)	4.68	6.65
Emittance (nmrad)	0.157 (AC, w/o undulators) ~ 0.10 (AC, w undulators)	2.4 (NA, w/o undulators)

Earliest Time Schedule

Fiscal Year	~2019	2020	2021
Existing SPring-8 Operation	Existing SPring-8 Operation	Blackout	SPring-8-II
Component Manufacturing & Integration into sub-systems	→		
Old Comp. Removal & New Comp. Inst., Cabling, Alignment, etc.		Dismantlement, Installation, Alignment, Evacuation	System Operation Test
Beam commissioning & fully outgassed			→

User Operation Start

Overview of SPring-8-II

	SPring-8-II	SPring-8
Beam Energy (GeV)	6	8
Ring Current (mA)	200	100
Unit-cell Structure	5-Bend Achromat	Double-Bend
Length of ID straight (m)	4.68	6.65
Emittance (nmrad)	0.157 (AC, w/o undulators) ~ 0.10 (AC, w undulators)	2.4 (NA, w/o undulators)

Earliest Time Schedule

Fiscal Year	~2019	2020	2021
	Existing SPring-8 Operation	Blackout	SPring-8-II
Component Manufacturing & Integration into sub-systems			
Old Comp. Removal & New Comp. Inst., Cabling, Alignment, etc.		Dismantlement, Installation, Alignment, Evacuation	System Operation Test
Beam commissioning & fully outgassed			User Operation Start

Overview of SPring-8-II

	SPring-8-II	SPring-8
Beam Energy (GeV)	6	8
Ring Current (mA)	200	100
Unit-cell Structure	5-Bend Achromat	Double-Bend
Length of ID straight (m)	4.68	6.65
Emittance (nmrad)	0.157 (AC, w/o undulators) ~ 0.10 (AC, w undulators)	2.4 (NA, w/o undulators)

Another project of constructing a new 3 GeV synchrotron facility is being promoted in Japan.

Features of Vacuum System

- ➢ Time constraint issue (1-year blackout for replacement of ***1.5 km storage ring***)
- ➢ Space constraint issue (Increase in number of multi-pole magnets and MBA)

1. *12-m-Long Integrated Chamber (12m-LIC)*

- ✓ The 12m-LIC has a welded integral structure with removing flanges as much as possible, which makes the longitudinal space shorter.
- ✓ The 12m-LIC can be prepared off-line in advance with two transport gate valves at both ends, which enables us to realize the UHV system in the ring tunnel within a limited period of time without exposing the vacuum surface to the air.

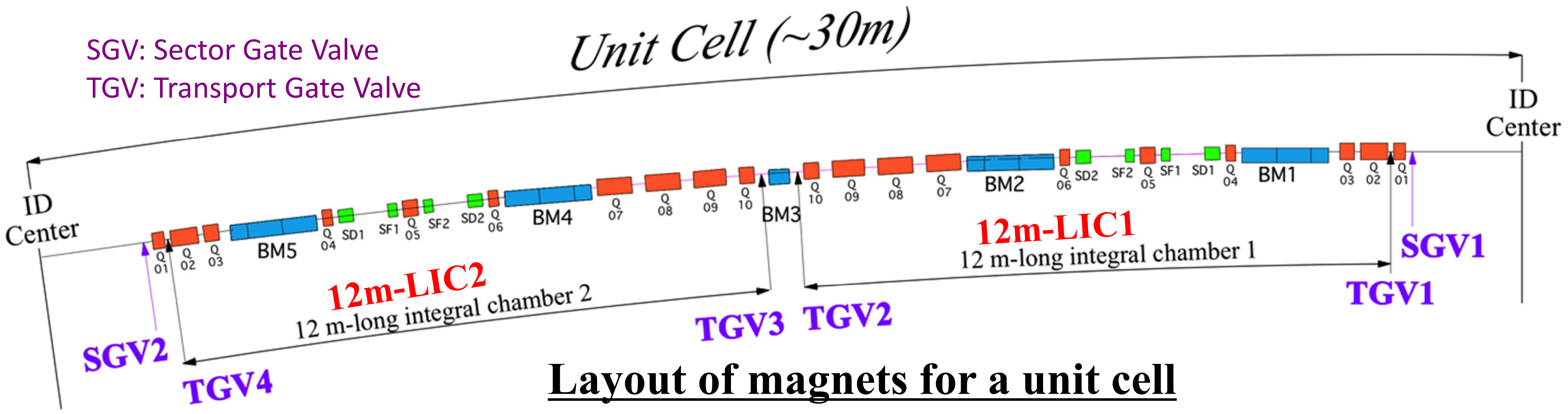

Layout of magnets for a unit cell

Features of Vacuum System

- ➢ Time constraint issue (1-year blackout for replacement of ***1.5 km storage ring***)
- ➢ Space constraint issue (Increase in number of multi-pole magnets and MBA)

1. 12-m-Long Integrated Chamber (12m-LIC)

- ✓ The 12m-LIC has a welded integral structure with removing flanges as much as possible, which makes the longitudinal space shorter.
- ✓ The 12m-LIC can be prepared off-line in advance with two transport gate valves at both ends, which enables us to realize the UHV system in the ring tunnel within a limited period of time without exposing the vacuum surface to the air.

SGV: Sector Gate Valve
TGV: Transport Gate Valve

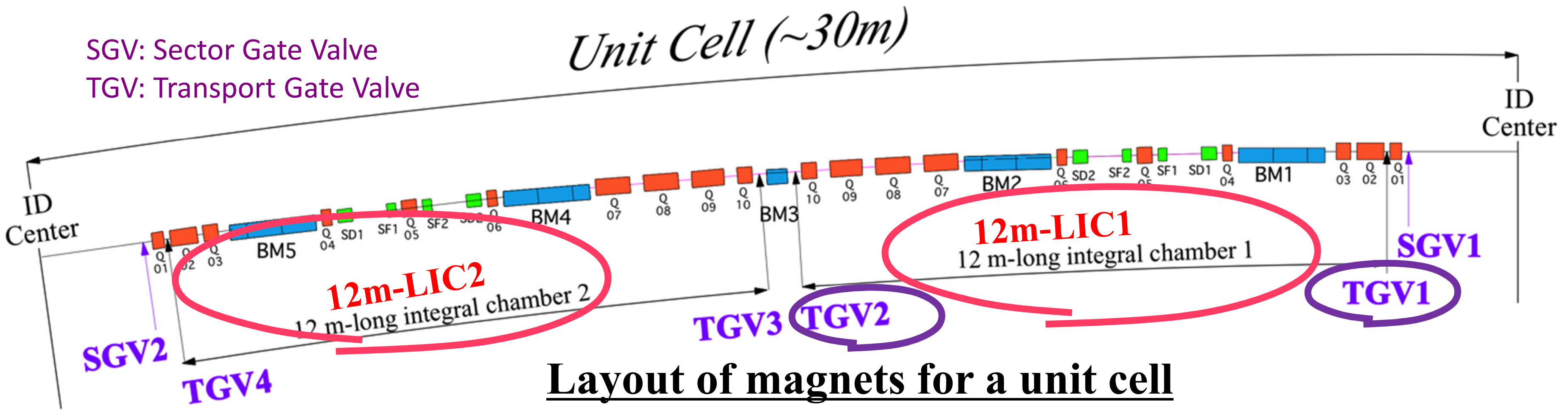

Layout of magnets for a unit cell

2. Compact Photon Absorbers

- ➢ Discrete type with a combination of conventional cartridge type NEG pump and ion pump locally so that the gas source could be localized and effective evacuation could be provided.

Vacuum Chamber

Main chamber material:

Proven Extruded Aluminum Alloy ⟶ *Stainless Steel (SS316L)*

- ➢ *Reducing the chamber thickness*
  => expansion of clearance between chamber and magnetic pole
- ➢ *Elimination of aluminum-SS transition space*
  => mitigation of packing factor in the longitudinal direction
- ➢ *Low outgassing rate*
  => increase in intervals between NEG reactivation

Test Production of SSC:

We tried to manufacture a straight section chamber (SSC), aiming at the similar cost in the case of using extruded aluminum alloy.

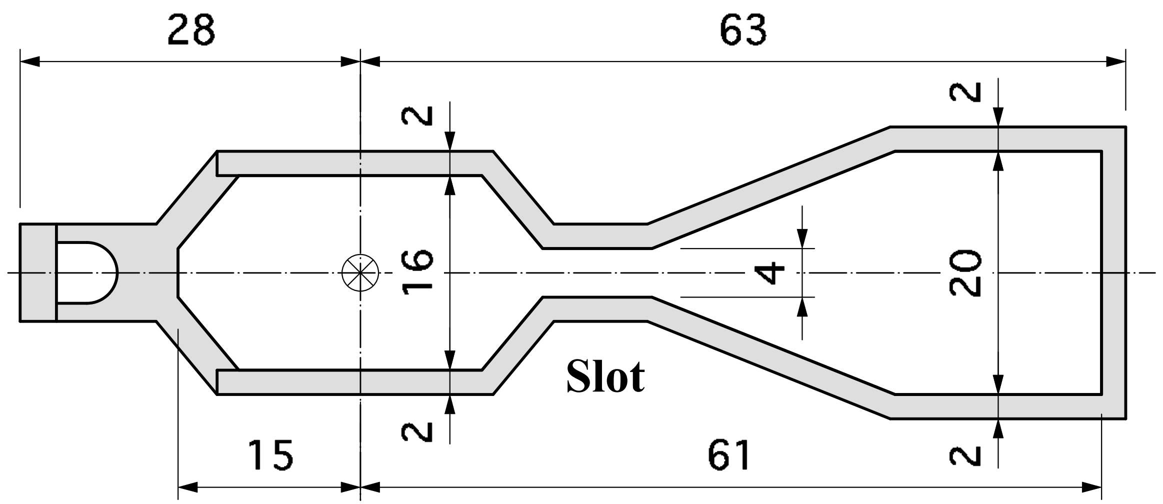

Height of slot:
4 mm ~ 9 mm corresponding to the magnetic pole dimension and vertical spread of the photon beam.

Cross-Sectional Drawing of Straight Section Chamber (SSC)

Test Production of SSC

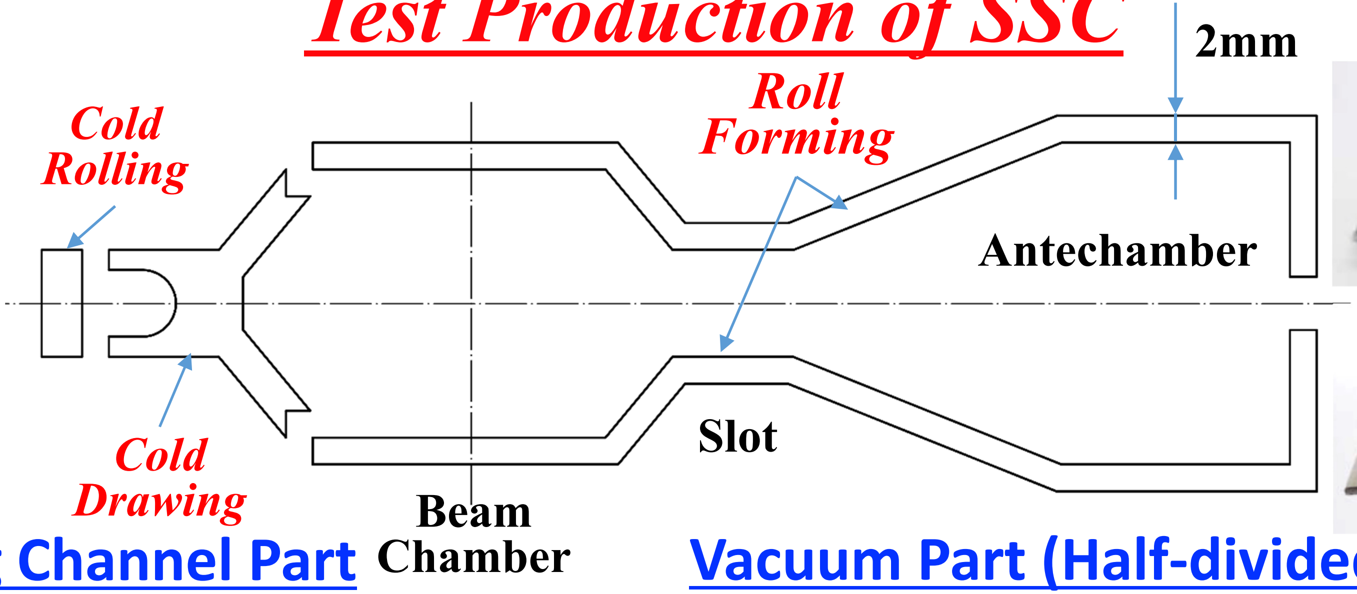

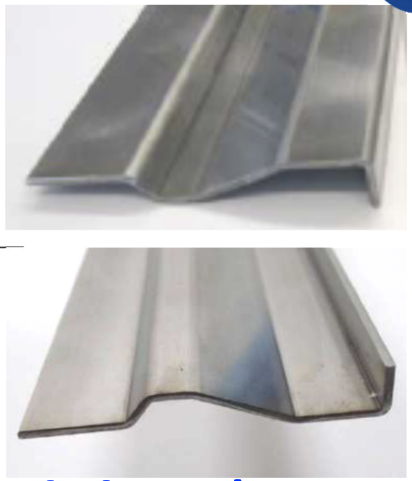

Cooling Channel Part

Vacuum Part (Half-divided shape)

Test Production of SSC

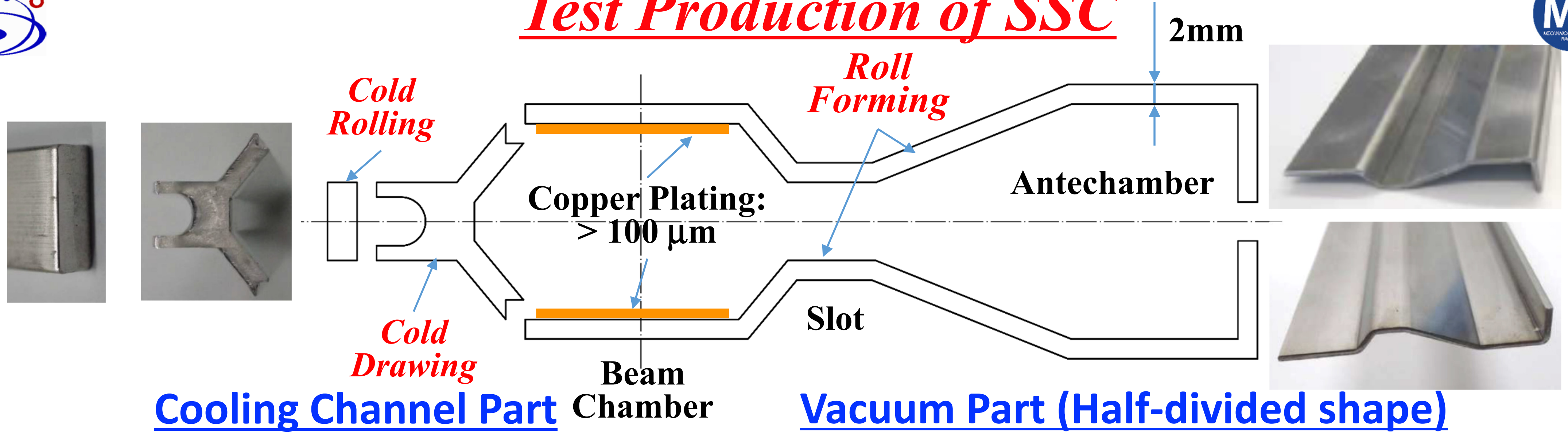

Cooling Channel Part

Vacuum Part (Half-divided shape)

Test Production of SSC

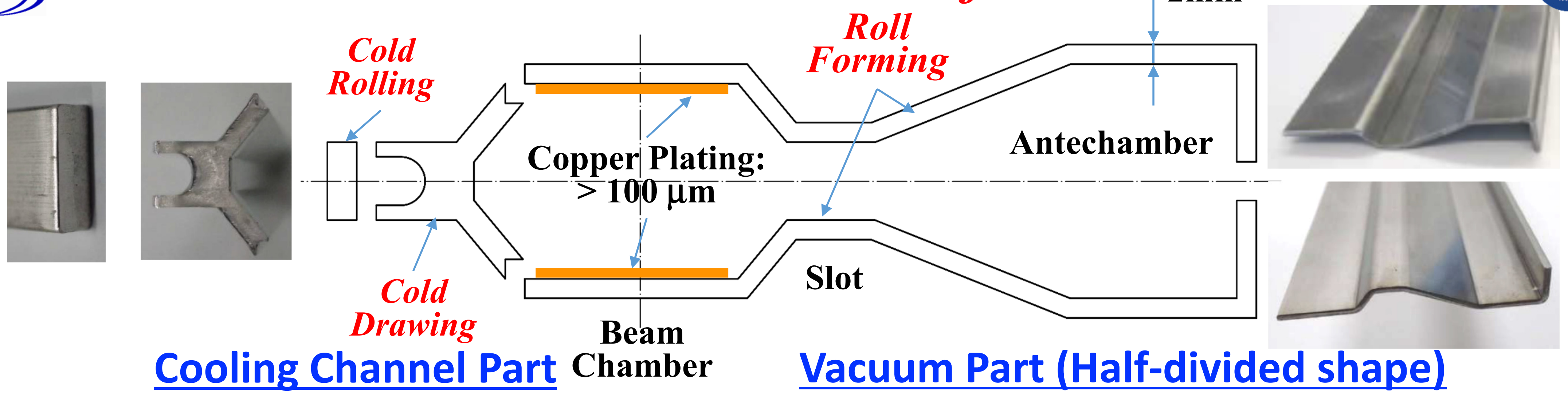

- Roll-forming is the best choice for mass production, because once the desired profile is obtained by adjusting sets of rolls appropriately, it can produce constant-profile parts continuously at high machining speed with high accuracy.
- A seam weld line tracking device is indispensable for efficient LBW.
- Copper plating on welding grooves should be removed completely before LBW.

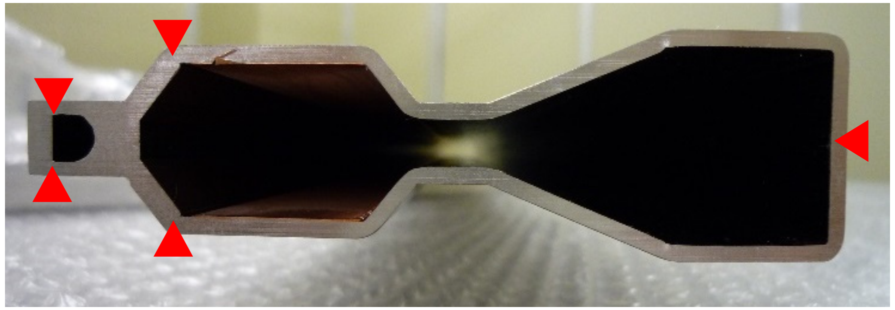

▼ : Laser Beam Welding Part
(small amount of heat input)

Chemical Polishing Treatment & Vacuum Annealing (>900ºC, >10min)

Manufacturing Accuracy	: Bend in the horizontal direction	< 1.8 mm/2 m
	: Bend in the vertical direction and twisting	< ± 0.5 mm
	: Cross-sectional deformation except both end	< ± 0.5 mm
Relative permeability	: <1.02 (after annealing)	

Almost acceptable,
but will be improved.

Distribution of Photon Absorbers

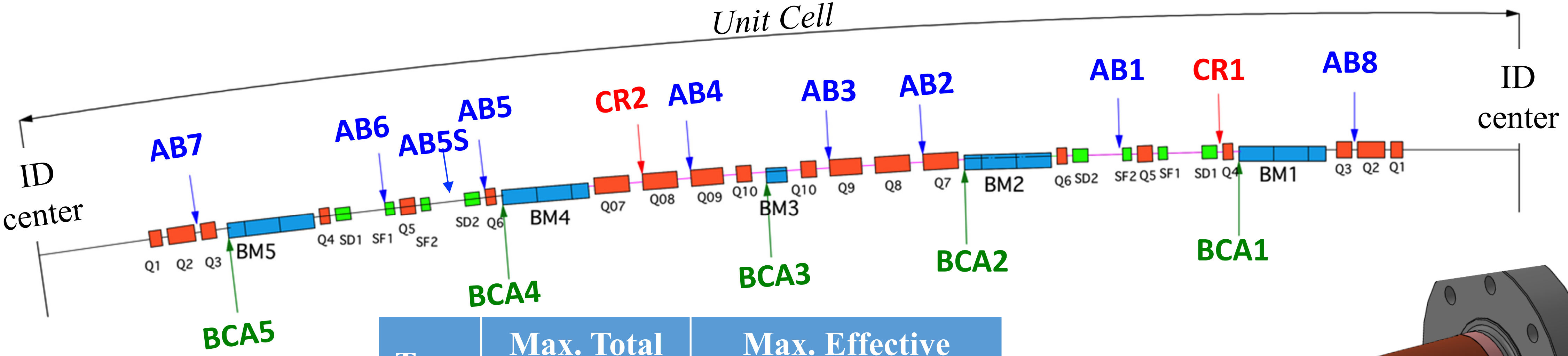

Type	Max. Total Power	Max. Effective Power Density
VIT	1.4 kW	*370* W/mm^2
HIT	0.8 kW	70 W/mm^2

Maximum heat load @200 mA operation

Existing SPring-8
>340 W/mm^2

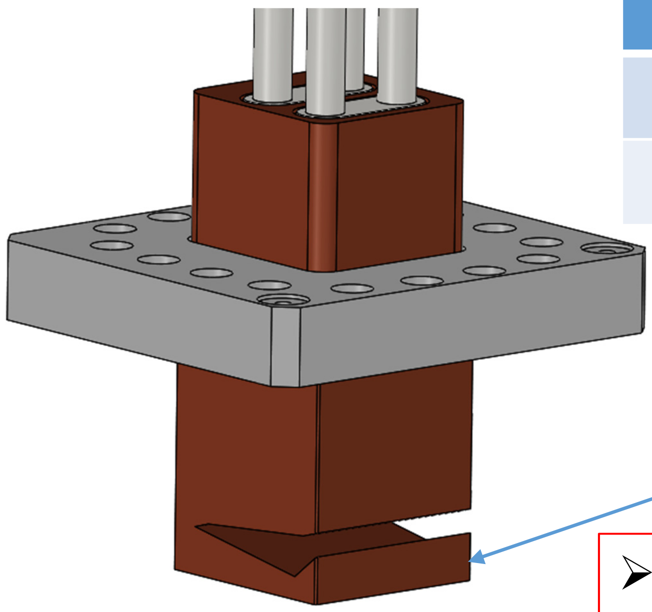

Vertical Insertion Type (VIT) for CR and AB

Scattering Blocking Structure

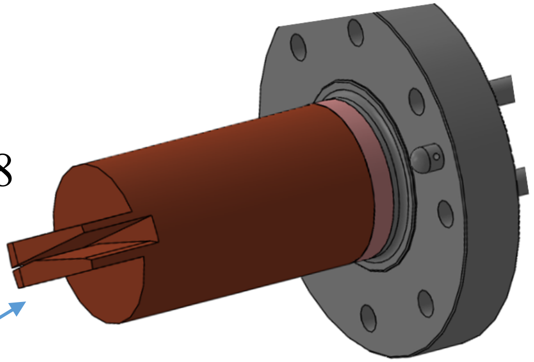

Horizontal Insertion Type (HIT) for BCA

<Design Guideline>

- Simple grazing angle technology at low cost.
- Scattering blocking structure.
- Double-tube configuration for cooling water system.

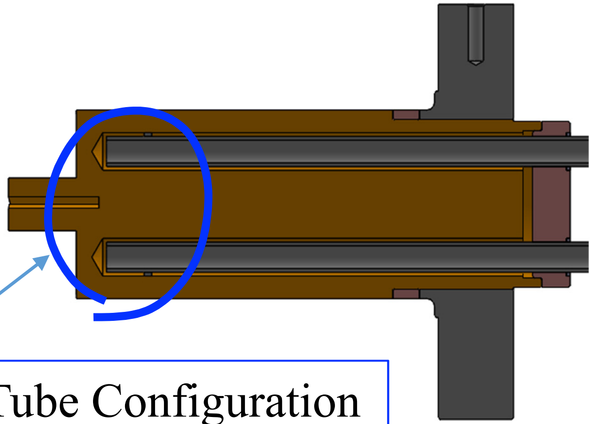

Double-Tube Configuration

Scattering Blocking Structure

- Due to the low thermal conductivity of stainless steel chamber, all the photon absorbers were equipped with a lower jaw for blocking the scattering in order to restrain the temperature of the surrounding chamber from rising.
- The energy escaping from the photon absorber (depositing on the surrounding vacuum chamber) was evaluated quantitatively in the case of AB5 by employing PHITS with EGS5 mode.

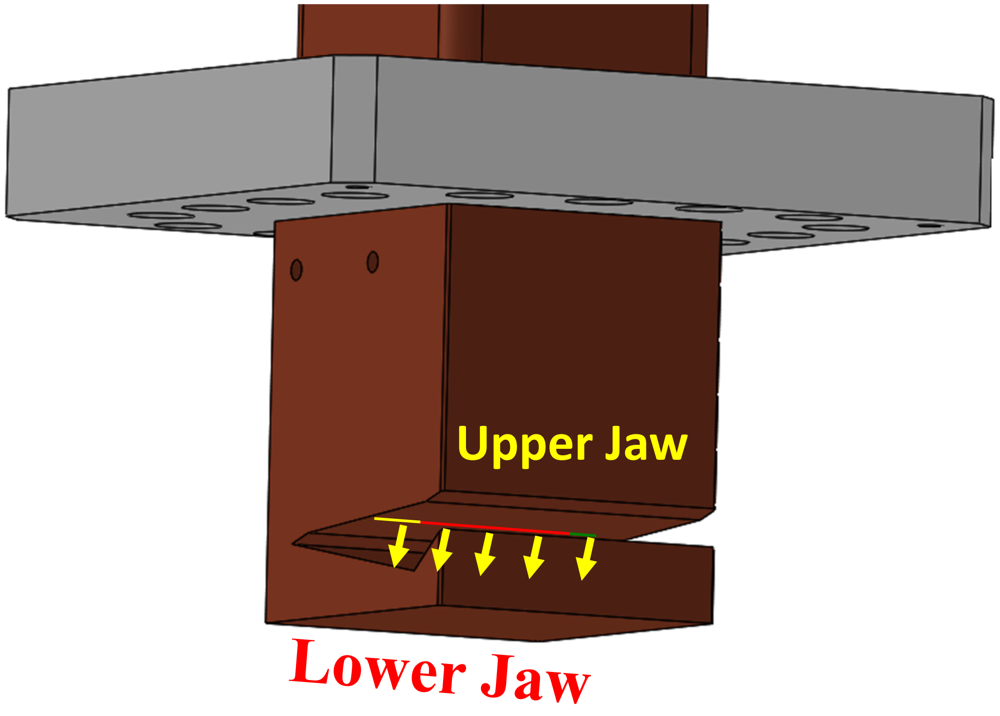

VIT (AB5)

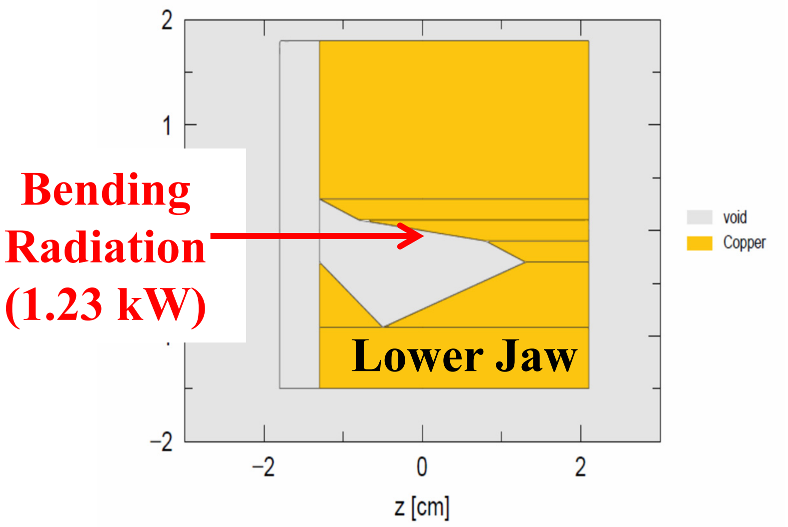

- ✓ Escaping from AB5: less than 1% (12 W)
- ✓ Depositing on the lower jaw: 3.6% (44 W)

Without Lower Jaw

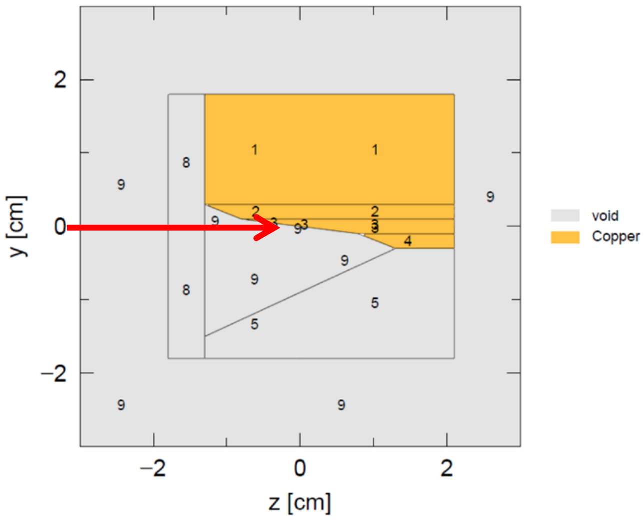

- ✓ Escaping from AB5: 6.2% (76 W)

Estimation of Heat Transfer Coefficient (HTC) by CFD Analysis

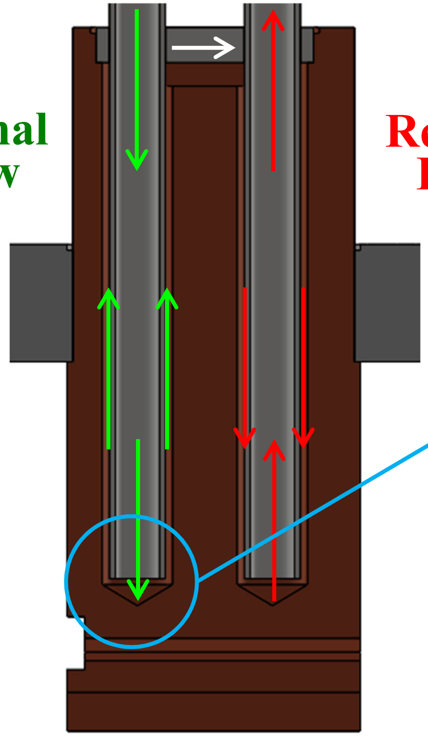

Sectional View of Double-Tube Cooling Channel in VITs

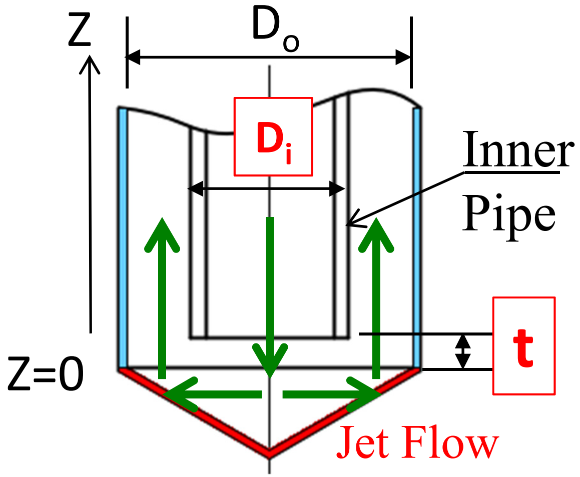

Flow Direction of Normal Flow

Normal Flow:
Cooling water is fed from the top of inner pipe and flows out through annular space.

$$Nu = \frac{HTC}{\lambda} = \frac{(f/2)\cdot(R_e - 1000)\cdot P_r}{1 + 12.7\cdot(f/2)^{0.5}\cdot(P_r^{2/3} - 1)}$$

Gnielinski Correlation (wide application range of Re)

$Re = \rho \cdot u \cdot d/\mu$ d: characteristic length

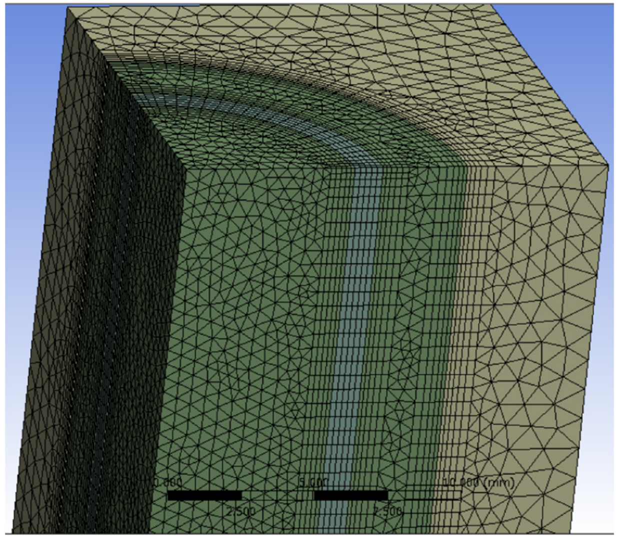

Meshed Quarter Model

- In general, heat Transfer Coefficient (HTC) in annulus duct in region of the turbulent flow is assumed by some empirical correlations, only applicable to fully developed turbulent flow in a circular tube, for example, the Gnielinski correlation.
- However, the influence of jet flow on the bottom and in the vicinity should be considered.
- ***The spatial distribution of HTC*** was calculated with ***pressure loss*** by means of CFD analysis, with parameterizing ***pipe size***, ***flow rate***, ***inserting depth of the inner pipe*** (t), and ***flow direction*** (normal or reverse).

Estimation of Heat Transfer Coefficient by CFD analysis

Do=12mm, Di=9.53mm & 5L/m

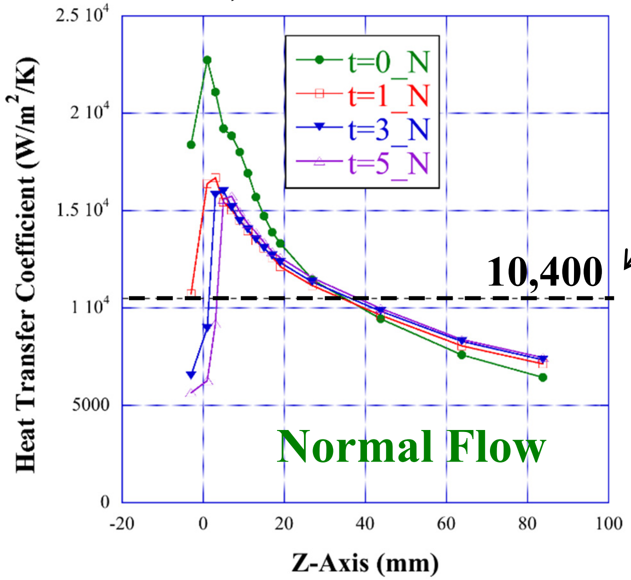

Calculated value from the Gnielinski correlation

The maximum HTC appeared on the wall around the inserting depth, and continued to decrease gradually toward the outlet.

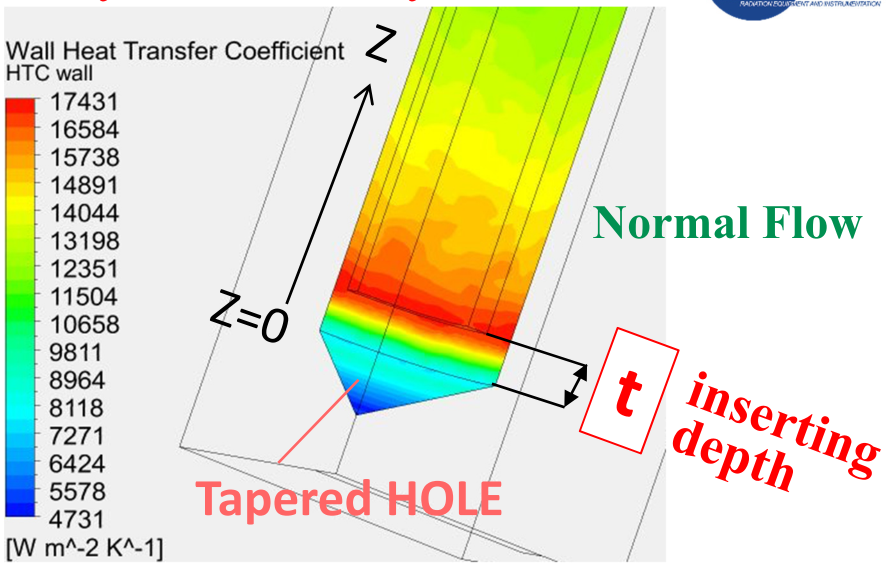

Contour Plot of HTC on Outer Wall of Annulus duct

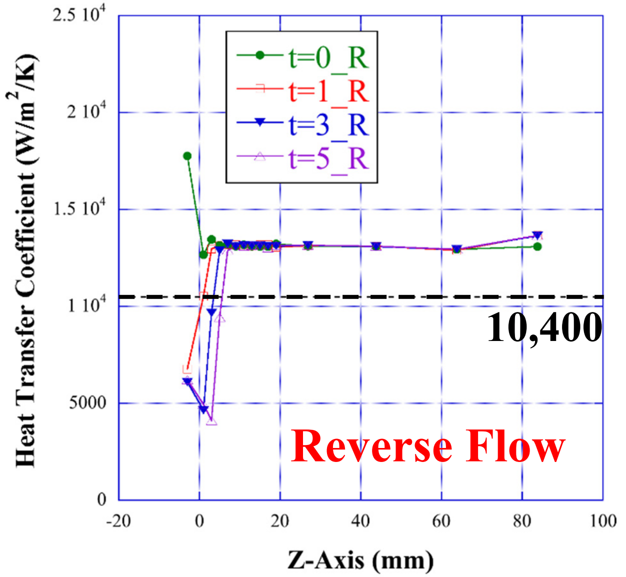

Except when the inserting depth equals to 0, HTC on the wall between the tapered hole and the bottom of the inner pipe was very small, but after that almost constant.

Do=12mm, Di=9.53mm & 5L/m

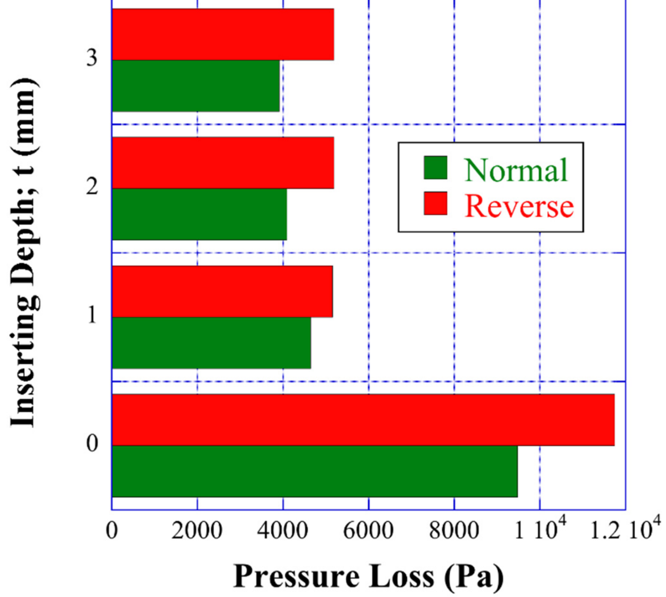

HTC Distribution along the Z-axis

Pressure Loss of each flow direction

Estimation of Heat Transfer Coefficient by CFD analysis

Do=12mm, Di=9.53mm & 5L/m

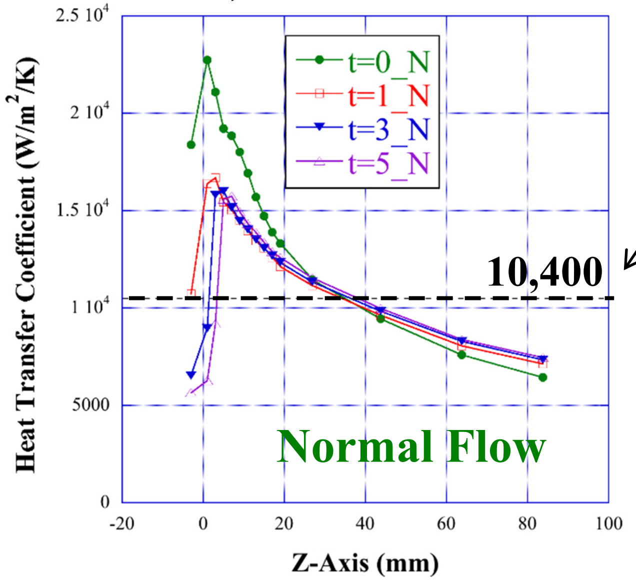

Calculated value from the Gnielinski correlation

The maximum HTC appeared on the wall around the inserting depth, and continued to decrease gradually toward the outlet.

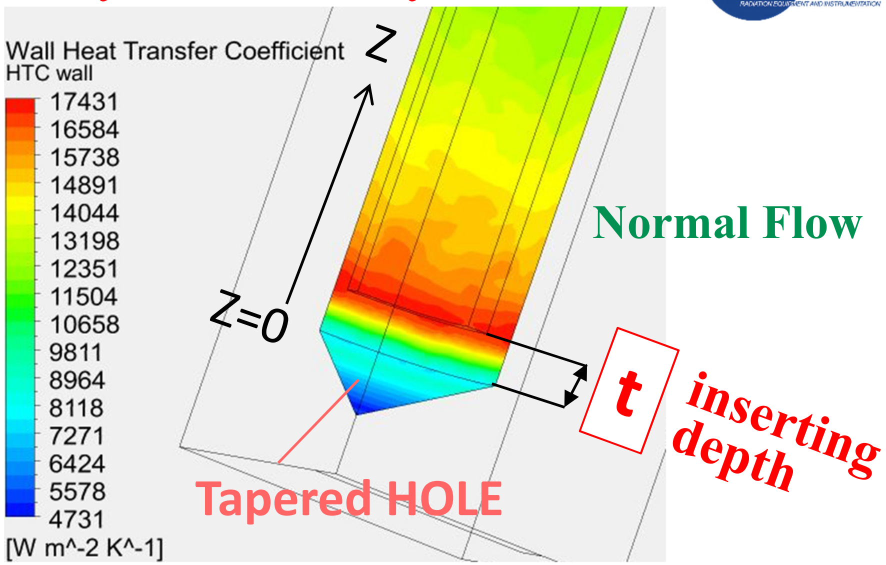

Contour Plot of HTC on Outer Wall of Annulus duct

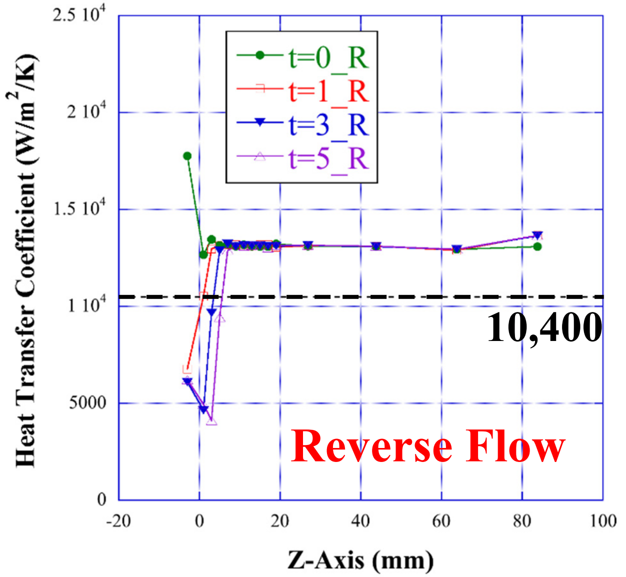

HTC Distribution along the Z-axis

Except when the inserting depth equals to 0, HTC on the wall between the tapered hole and the bottom of the inner pipe was very small, but after that almost constant.

Based on both results, the inserting depth should be put as close as possible to 0, if the pressure loss is within an allowable range.

Do=12mm, Di=9.53mm & 5L/m

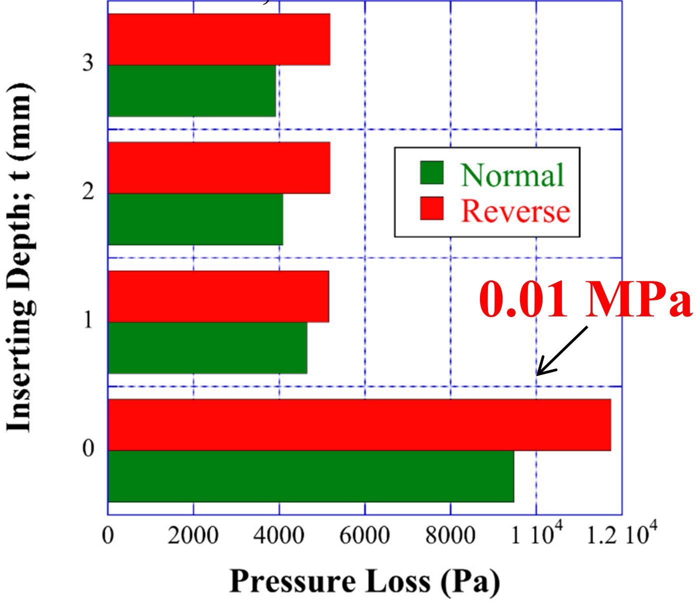

Pressure Loss of each flow direction

Example of Thermo-Mechanical Analysis

AB4

TP: 1.4 kW
PPD: 370 W/mm²
@200 mA

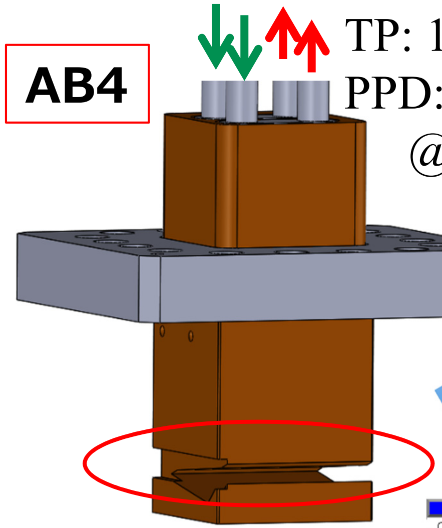

Material: Glidcop AL15 (heat treatment @ 1010ºC)

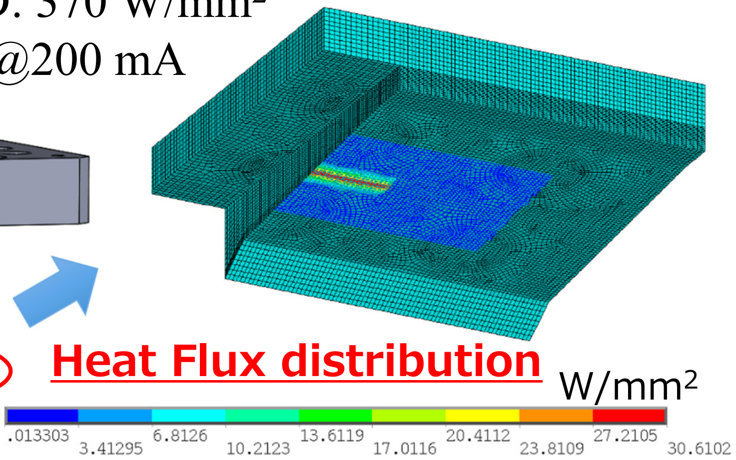

Heat Flux distribution W/mm²

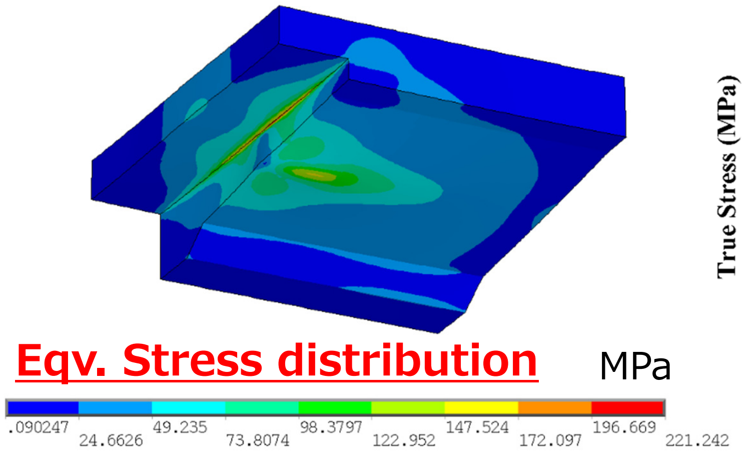

Eqv. Stress distribution MPa

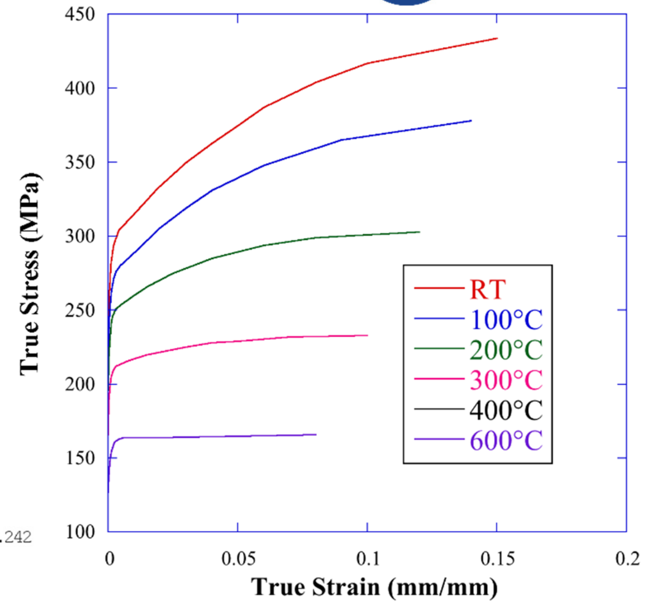

Stress-Strain diagrams in plastic strain region

CASE	Max. Temp. (°C)		Thermo-Mechanical	
	Body	Cooling Surface	Eqv. Stress (MPa)	Eqv. Plastic Strain (%)
On-Axis	283.2	83.3	221	—
Off-Axis_up	288.4	120.3	228	—
Off-Axis_low	290.4	104.0	180	—

Off-Axis: Beam position deviates by ±0.8 mm from the center in the vertical direction.

<Boundary Condition>
The spatial distribution of HTC from CFD analysis was set on the cooling surfaces on condition that t=1 mm for safer side estimation.

Design Criteria

- ✓ Max. Body Temp. : less than 300ºC
- ✓ Max. Cooling Surface Temp.:
  On-Axis: less than 100ºC
  Off-Axis: less than the boiling point

- ✓ Not allowing "Plastic Deformation"

We have a prospect of designing an absorbing body capable of handling the heat load corresponding to 200 mA operation.

Test Half-Cell Construction

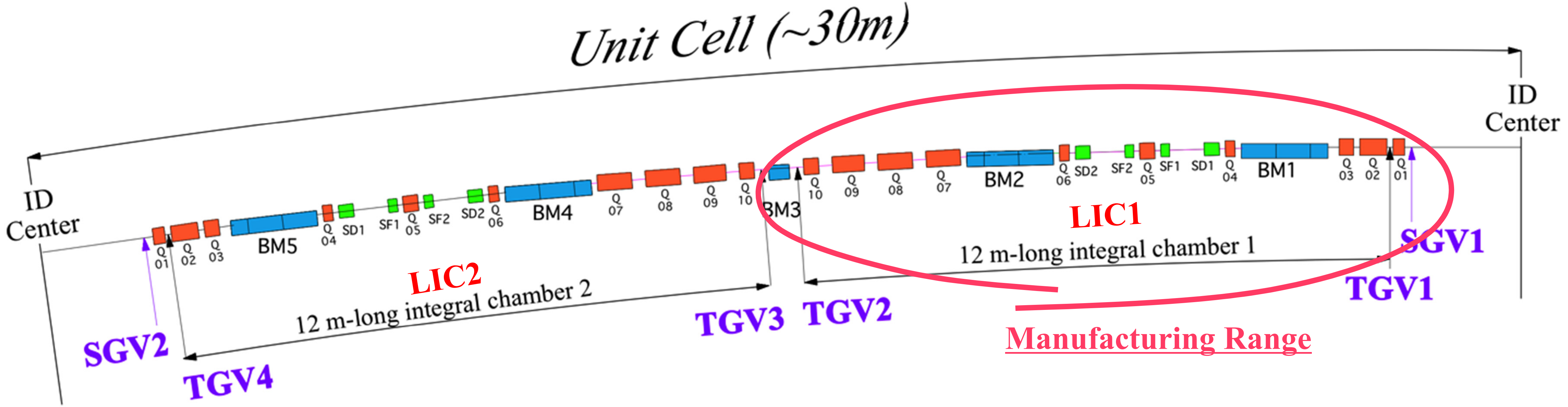

- Underway and scheduled for completion in summer of 2018.
- Test half-cell construction includes 12m-LIC, magnets on a common girder, and monitors.
- To confirm interference between sub-systems and consistency in the strategy for installation and alignment.

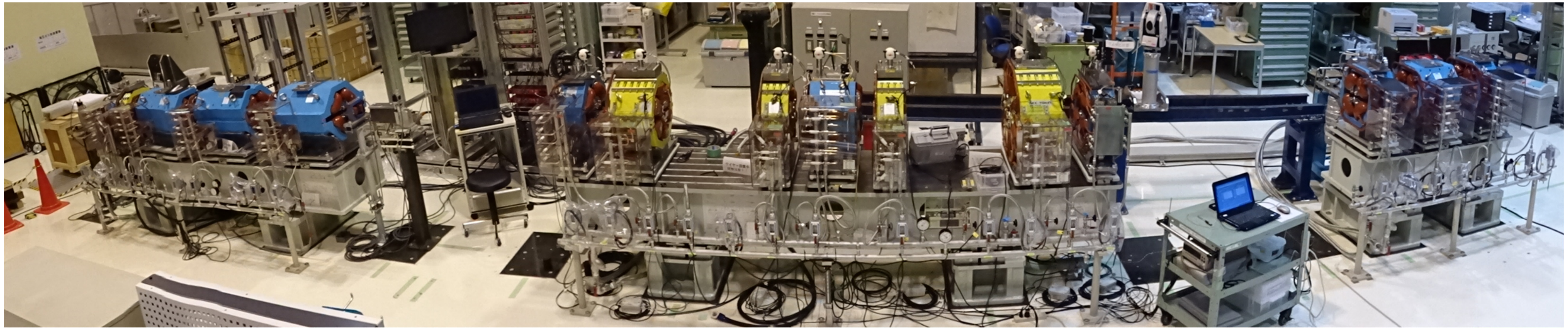

Prototype of 12m-LIC for Test Half-Cell Construction

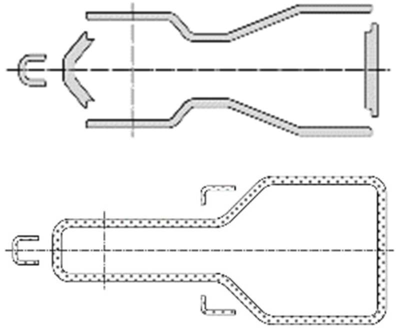

Chamber parts

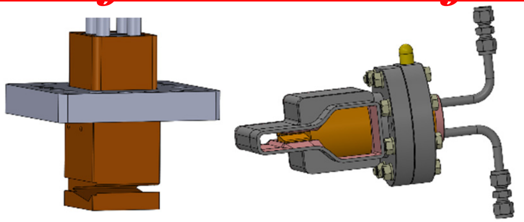

Photon Absorber parts

NEG, SIP, Bellows ···
Vacuum Components

Unitization

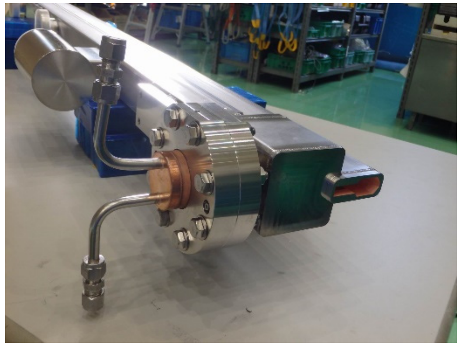

Unitized Straight Section Chamber (U-SSC)
Unitized Bending Section Chamber (U-BSC)
U-SSC with Photon Duct

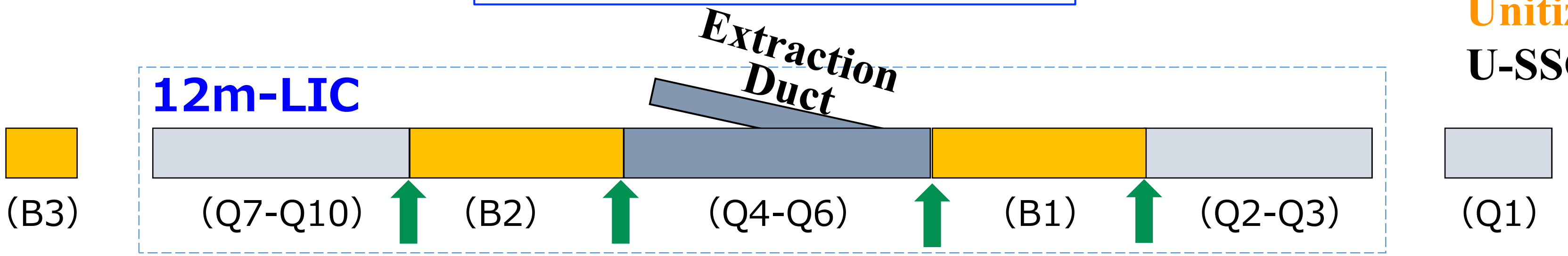

Assembled for 12m-LIC

U-SSC | U-BSC | U-SSC with Photon Duct | U-BSC | U-SSC

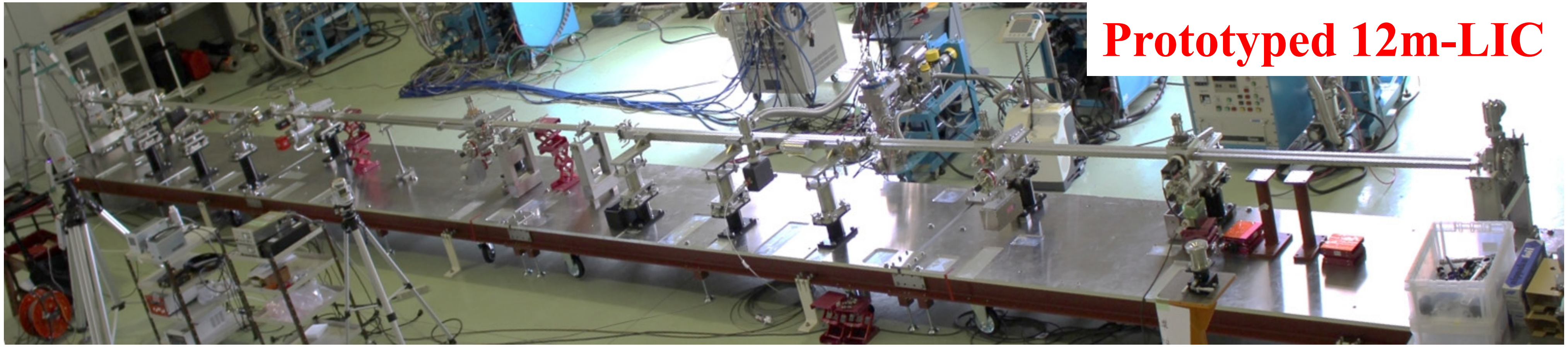

Prototyped 12m-LIC

Hot-Air Baking and NEG Activation

Target temperature
=> 150ºC

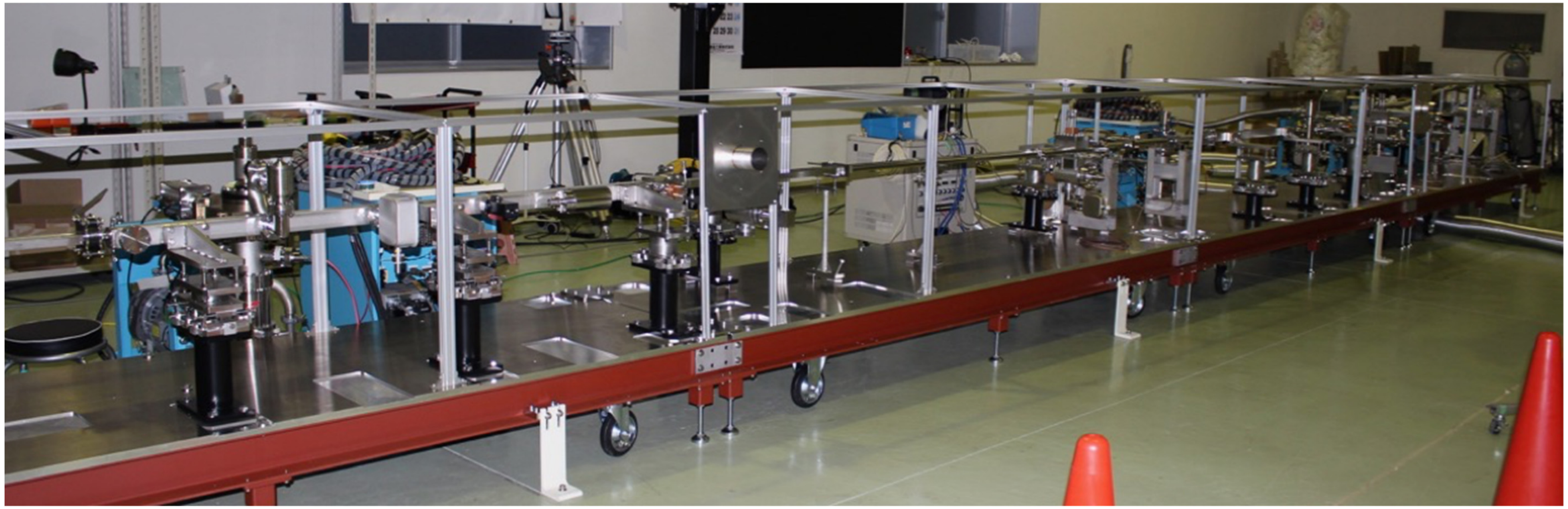

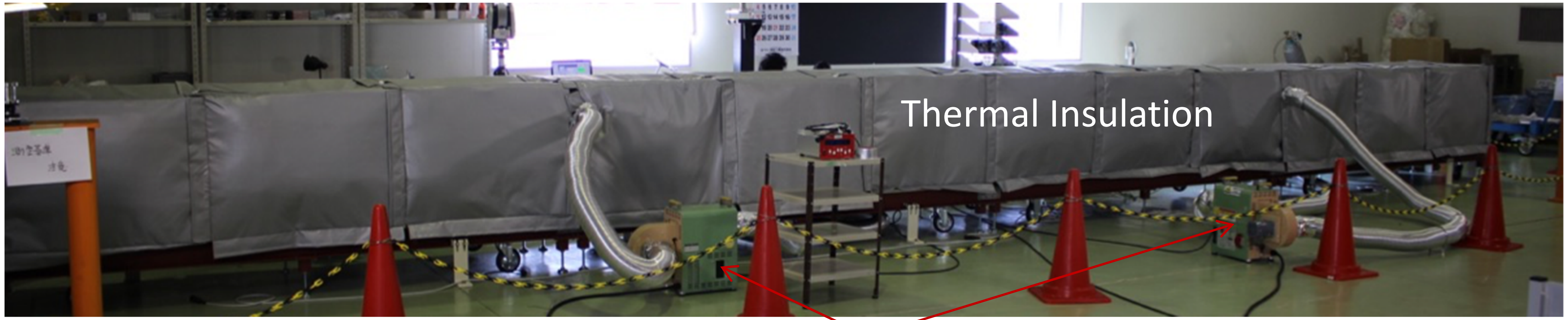

Hot-Air Fryer

- The cross-sectional area of the frame was so hollow that the hot-air volume could not be sufficient, leading to unevenness of temperature.
- The final pressure was confirmed to be of the order of 10^{-8} Pa after NEG activation.

Transportation to Ring Tunnel (for Installation Test)

Suspending Tool

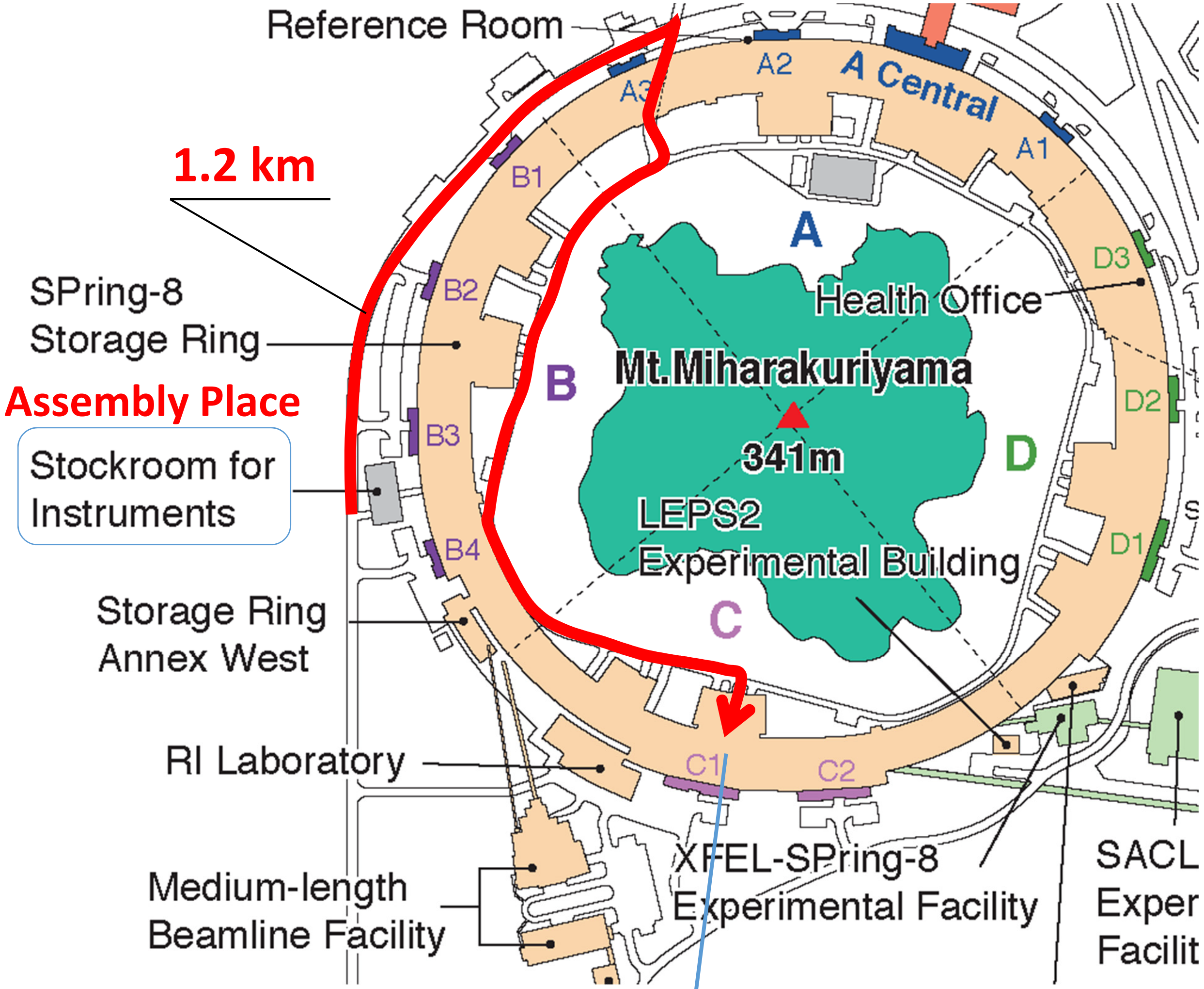

Equipment Carrying-in Entrance (C)

Unloading at Equipment Carrying-in Entrance of Ring Tunnel

Hoisting in the Ring Tunnel

Summary

1. In Japan, a new 3 GeV synchrotron facility construction project with a higher priority has come up and this situation delayed the start of SPring-8-II (6 GeV) by several years.
2. Results of R&D for SPring-8-II, including related to the vacuum system, are going to be applied for the 3 GeV project.
3. We have mostly succeeded in manufacturing, transporting, and installing 12m-LIC made of stainless steel, which is the key component for the vacuum system.
4. As to the photon absorbers, we have a prospect of designing a heat absorbing body capable of handling the heat load corresponding to 6 GeV/200 mA & 3 GeV/500 mA operation.